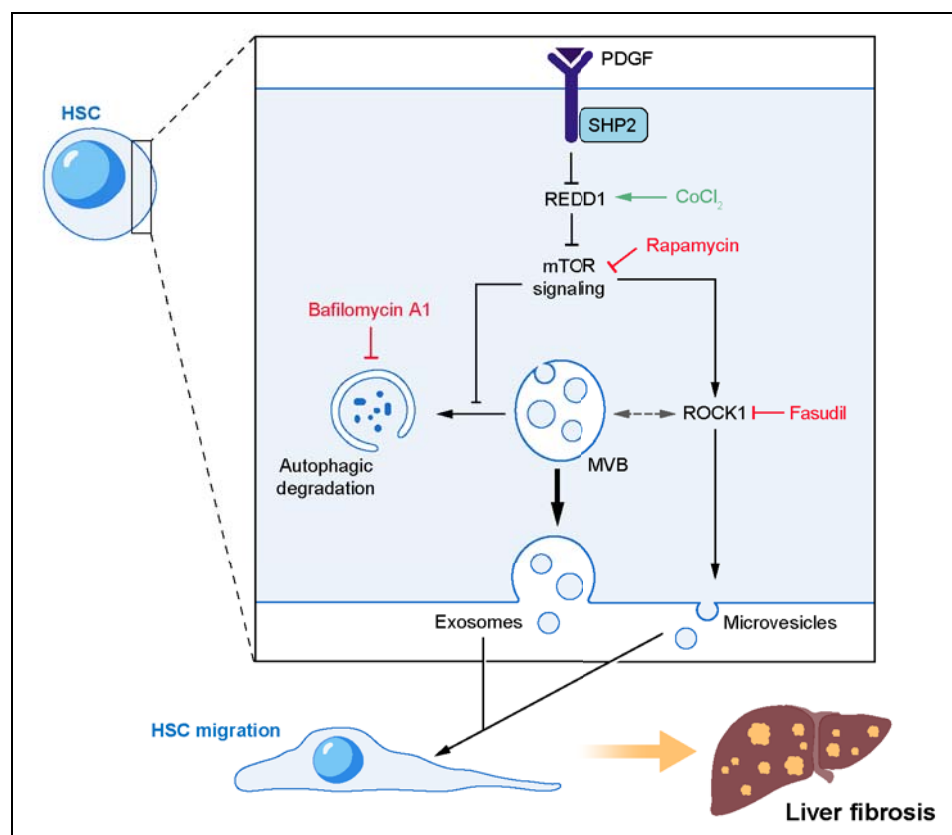


Hepatic stellate cell autophagy inhibits extracellular vesicle release to attenuate liver fibrosis

Graphical abstract



Authors

Jinhang Gao, Bo Wei, Thiago M. de Assuncao, ..., Sheng Cao, Vijay H. Shah, Enis Kostallari

Correspondence

kostallari.enis@mayo.edu,
enis.kostallari@gmail.com
(E. Kostallari).

Lay summary

During liver fibrosis and cirrhosis, activated hepatic stellate cells (HSCs) are the key cell type responsible for fibrotic tissue deposition. Recently, we demonstrated that activated HSCs release nano-sized vesicles enriched with fibrogenic proteins. In the current study, we unveil the mechanism by which these fibrogenic vesicles are released, moving a step closer to the long-term goal of therapeutically targeting this process.

Highlights

- PDGF and SHP2 induce fibrogenic EV release by activating mTOR signaling.
- mTOR signaling inhibits autophagy, leading to the release of MVB content as exosomes.
- mTOR signaling activates ROCK signaling, leading to the release of microvesicles.
- Blocking this mechanism inhibits the circulation of pro-fibrotic exosomes and microvesicles, and thus fibrosis in mice.



Hepatic stellate cell autophagy inhibits extracellular vesicle release to attenuate liver fibrosis

Jinhang Gao^{1,2}, Bo Wei^{1,2}, Thiago M. de Assuncao¹, Zhikui Liu¹, Xiao Hu¹, Samar Ibrahim¹,
Shawna A. Cooper^{1,3}, Sheng Cao¹, Vijay H. Shah¹, Enis Kostallari^{1,*}

¹Division of Gastroenterology and Hepatology, Mayo Clinic, Rochester, MN, United States; ²Gastroenterology and Hepatology, West China Hospital, Sichuan University, Chengdu, 610041 China; ³Biochemistry and Molecular Biology Graduate Program, Mayo Clinic Graduate School of Biomedical Sciences, Mayo Clinic, Rochester, MN, United States

Background & Aims: Autophagy plays a crucial role in hepatic homeostasis and its deregulation has been associated with chronic liver disease. However, the effect of autophagy on the release of fibrogenic extracellular vesicles (EVs) by platelet-derived growth factor (PDGF)-stimulated hepatic stellate cells (HSCs) remains unknown. Herein, we aimed to elucidate the role of autophagy, specifically relating to fibrogenic EV release, in fibrosis.

Methods: *In vitro* experiments were conducted in primary human and murine HSCs as well as LX2 cells. Small EVs were purified by differential ultracentrifugation. Carbon tetrachloride (CCl₄) or bile duct ligation (BDL) were used to induce fibrosis in our mouse model. Liver lysates from patients with cirrhosis or healthy controls were compared by RNA sequencing.

Results: *In vitro*, PDGF and its downstream molecule SHP2 (Src homology 2-containing protein tyrosine phosphatase 2) inhibited autophagy and increased HSC-derived EV release. We used this PDGF/SHP2 model to further investigate how autophagy affects fibrogenic EV release. RNA sequencing identified an mTOR (mammalian target of rapamycin) signaling molecule that was regulated by SHP2 and PDGF. Disruption of mTOR signaling abolished PDGF-dependent EV release. Activation of mTOR signaling induced the release of multivesicular body-derived exosomes (by inhibiting autophagy) and microvesicles (by activating ROCK1 signaling). These mTOR-dependent EVs promoted *in vitro* HSC migration. To assess the importance of this mechanism *in vivo*, SHP2 was selectively deleted in HSCs, which attenuated CCl₄ or BDL-induced liver fibrosis. Furthermore, in the CCl₄ model, mice receiving circulating EVs derived from mice with HSC-specific *Shp2* deletion had less fibrosis than mice receiving EVs from control mice. Correspondingly, SHP2 was upregulated in patients with liver cirrhosis.

Conclusion: These results demonstrate that autophagy in HSCs attenuates liver fibrosis by inhibiting the release of fibrogenic EVs.

Lay summary: During liver fibrosis and cirrhosis, activated hepatic stellate cells (HSCs) are the key cell type responsible for

fibrotic tissue deposition. Recently, we demonstrated that activated HSCs release nano-sized vesicles enriched with fibrogenic proteins. In the current study, we unveil the mechanism by which these fibrogenic vesicles are released, moving a step closer to the long-term goal of therapeutically targeting this process.

© 2020 European Association for the Study of the Liver. Published by Elsevier B.V. All rights reserved.

Introduction

Autophagy is a degradative process among eukaryotes in which double-membrane vesicles named autophagosomes fuse with lysosomes to degrade cytosolic proteins and organelles.¹ Autophagy contributes to liver homeostasis and its deregulation has been linked to several chronic liver diseases.^{2,3} The role of autophagy in liver disease depends on the cell type and the stage of the disease.^{2,4,5} In hepatocytes, autophagy has been demonstrated to have a protective role, while it has been proposed that autophagy in hepatic stellate cells (HSCs) might induce their activation through lipophagy, a selective type of lipid droplet degradation.² However, mammalian target of rapamycin (mTOR) – an inhibitor of autophagy – actually promotes HSC activation and liver fibrosis.^{6,7} Thus, deciphering the finely tuned mechanisms by which autophagy is involved in the amplification of fibrogenic signals is key to improving our understanding of liver fibrosis.

Extracellular vesicles (EVs) have emerged as important cell-derived particles in liver injury and fibrosis progression.⁸ Small EVs range from 50–150 nm, taking the form of ADP ribosylation factor 6 (Arf6)-enriched microvesicles or CD63- and CD81-enriched exosomes.⁸ EVs are significantly involved in cell-to-cell communication through delivery of diverse cargo.⁹ In the liver, EVs from injured hepatocytes and liver sinusoidal endothelial cells (LSECs) induce HSC activation and migration.⁸ Interestingly, EV release increases in response to liver injury,^{10–12} while inhibition of autophagy or lysosomal degradation have been associated with increased EV release.^{13,14} However, there is a lack of understanding of how pathogenic EVs are released and more specifically how autophagy may regulate the biogenesis of pro-fibrotic HSC-derived EVs.

One of the key molecules in the progression of liver fibrosis is platelet-derived growth factor (PDGF), released by LSECs, Kupffer cells and HSCs.¹⁵ PDGF is an essential tool for *in vitro* studies as it induces activation and migration of HSCs,¹⁶ the primary cell type involved in matrix deposition during fibrogenesis.¹⁷ In HSCs,

Keywords: Autophagy; Hepatic stellate cell; Exosome; Microvesicle; mTOR signaling; Liver fibrosis.

Received 18 November 2019; received in revised form 29 April 2020; accepted 30 April 2020; available online 8 May 2020

* Corresponding author. Address: Mayo Clinic, 200 First Street, SW, Rochester, MN 55905. Tel.: +15072669015.

E-mail addresses: kostallari.enis@mayo.edu, enis.kostallari@gmail.com (E. Kostallari).
<https://doi.org/10.1016/j.jhep.2020.04.044>



ELSEVIER

PDGF binding to PDGF receptor (PDGFR) induces tyrosine autophosphorylation which recruits important downstream signaling molecules, such as Src homology 2 domain protein phosphatase 2 (SHP2).¹⁸ Recently, fibroblastic SHP2 has been shown to induce skin and lung fibrosis.¹⁹ Previously, we demonstrated that PDGF and SHP2 promote enrichment of HSC-derived EVs with fibrogenic proteins.²⁰ Based on this, we used this PDGF/SHP2 model as a platform to study the role of autophagy in the field of HSC-derived EV release and liver fibrosis.

In the present study, we demonstrate that HSCs release EVs through mTOR by inhibiting autophagy and activating Rho-associated protein kinase 1 (ROCK1) signaling. Moreover, this EV release mechanism participates in liver fibrosis progression. In conclusion, HSC autophagy reduced liver fibrosis by attenuating fibrogenic HSC-derived EV release.

Material and methods

In vivo experiments

In vivo protocols were approved by the Mayo Clinic Institutional Animal Care and Use Committee. In all *in vivo* experiments, mice received humane care and were sex and age matched. Six-week old wild-type (WT) C57Bl/6 mice were purchased from Envigo and transgenic mice from Jackson Laboratory. *Pdgfrb*^{CreERT2} (B6.Cg-Tg(*Pdgfrb-cre/Ert2*)6096Rha/J), *Shp2*^{fl/fl} (Ptpn11tm1.1Wbm/J) and Rosa26-Tomato-STOP-GFP (B6.129(Cg)-Gt(ROSA)26Sortm4(ACTB-tdTomato,-EGFP)Luo/J) mice were crossed in our facilities. Heterozygous *Pdgfrb*^{CreERT2}/*Shp2*^{fl/+} (*Shp2*^{Δ/+}) or homozygous *Pdgfrb*^{CreERT2}/*Shp2*^{fl/fl} (*Shp2*^{ΔHSC}) mice were obtained. For Cre efficiency, *Pdgfrb*^{CreERT2} mice were crossed with Rosa26-Tomato-STOP-GFP mice (B6.129(Cg)-Gt(ROSA)26Sortm4(ACTB-tdTomato,-EGFP)Luo/J). The Cre recombinase activity was stimulated by intraperitoneal administration of 75 mg/kg tamoxifen (Sigma-Aldrich #10540-29-1) for 5 consecutive days. There was a 2-week waiting period after the last tamoxifen injection prior to any experimentation. Carbon tetrachloride (CCl₄; 1 μl/g of body weight, Sigma-Aldrich #319961) was administered via intraperitoneal injection twice a week for 4–6 weeks. Bile duct ligation (BDL) or sham operations were performed as previously described²⁰; mice were sacrificed 3 weeks later. For EV transplantation, 2 × 10⁸ serum EVs/mouse/day were administered daily via intraperitoneal injections for 4 weeks. Livers were collected and analyzed by Sirius red and western blotting (WB).

Patients

Patient serum samples were obtained and analyzed under Mayo Clinic Institutional Review Board-approved protocols. Informed consent was obtained from all patients. Patient demographics are detailed in Table S1.

EV purification

EVs were purified using a differential ultracentrifugation method.²⁰ Briefly, equal volumes of 12 h conditioned media or serum across experimental conditions were centrifuged for 10 min at 300 g, 30 min at 20,000 g (big EVs) and 2.5 h at 120,000 g (small EVs) using Optima XPN-80 ultracentrifuge. Small EVs were resuspended in equal volumes for Nanoparticle-Tracking Analysis (NTA, NS300), WB or EV transplantation.

Imaging

A Zeiss Definite Focus .2 microscope with AxioCam 702 mono camera was used. For live cell imaging, cells were photographed

every 5 min for 4 h, ZEN2 (blue edition) was used for fluorescence quantification. For immunofluorescence stainings, ImageJ was utilized for image analysis.

Statistical analysis

Graphpad Prism software was used for statistical analysis. Normal distribution was examined utilizing Shapiro-Wilk test. ANOVA with Bonferroni post-test, Mann-Whitney *U* and *t* tests were used to analyze the data. The difference was considered significant for *p* values lower than 0.05. Results are presented as mean ± SEM. Sample size was determined using <https://www.sample-size.net/sample-size-means/>.

In vitro experiments, RNA sequencing, gene expression, WB, immunofluorescence, small interfering RNA (siRNA) knockdown, protein array and antibodies are described in the supplementary information and CTAT table.

Results

PDGF inhibits autophagy and increases EV release

We first aimed to test the hypothesis that in HSCs, PDGF stimulation inhibits autophagy and increases EV release. For this, we utilized an mCherry-eGFP-LC3b plasmid,²¹ which expresses mCherry-eGFP-LC3b chimeric protein, where LC3b (microtubule-associated proteins 1A/1B light chain 3B) is an autophagosome component, enabling detection of degrading vs. non-degrading autophagosomes (Fig. S1). Autophagosome-lysosome fusion for cargo degradation lowers the pH to eGFP signal extinction, while mCherry fluorescence stays constant. However, when autophagosomes do not fuse with lysosomes, they remain eGFP⁺ and mCherry⁺. LX2 cells (human hepatic stellate cell line) were transfected with mCherry-eGFP-LC3b plasmid and treated with vehicle, the autophagic degradation inhibitor bafilomycin A1 or PDGF. As predicted, compared to the vehicle (Fig. 1A left, Movie S1), treatment of the cells with bafilomycin A1 increased the eGFP⁺-mCherry⁺ autophagosome pool (yellow color) (Fig. 1A middle, Movie S2) leading to an increased yellow/red ratio (Fig. 1A graph) indicative of autophagy inhibition. Like bafilomycin A1, PDGF also increased the yellow/red ratio compared to basal media condition at 4 h of treatment (Fig. 1A right and graph, Movie S3), demonstrating for the first time that PDGF inhibited autophagic degradation.

Consistent with these results, PDGF treatment, but not transforming growth factor-β (TGFβ) treatment, of primary human HSCs increased the protein levels of LC3b and p62, both crucial for autophagosome formation (Fig. 1B left, Fig. S2). PDGF did not increase *LC3b* or *p62* mRNA levels (Fig. 1B, right), suggesting that the protein level increase was due to reduced autophagic degradation and not *de novo* expression. The PDGF-mediated inhibition of autophagy correlated with an increase of the CD63⁺ multivesicular body (MVB) pool in primary human HSCs (Fig. 1C) and an increase of EV release from primary human and mouse HSCs (Fig. 1D–E). One of the crucial downstream signaling molecules of PDGF is SHP2.¹⁸ Inhibition of SHP2 by the competitive inhibitor, SHP099, abolished PDGF-mediated EV release (Fig. 1D). SHP099 also decreased LC3b protein levels (Fig. 1F) suggesting that SHP2 inhibition promoted autophagic degradation. These results support the concept that PDGF signaling in HSCs inhibits autophagy and increases EV release, suggesting that autophagy may inhibit EV release.

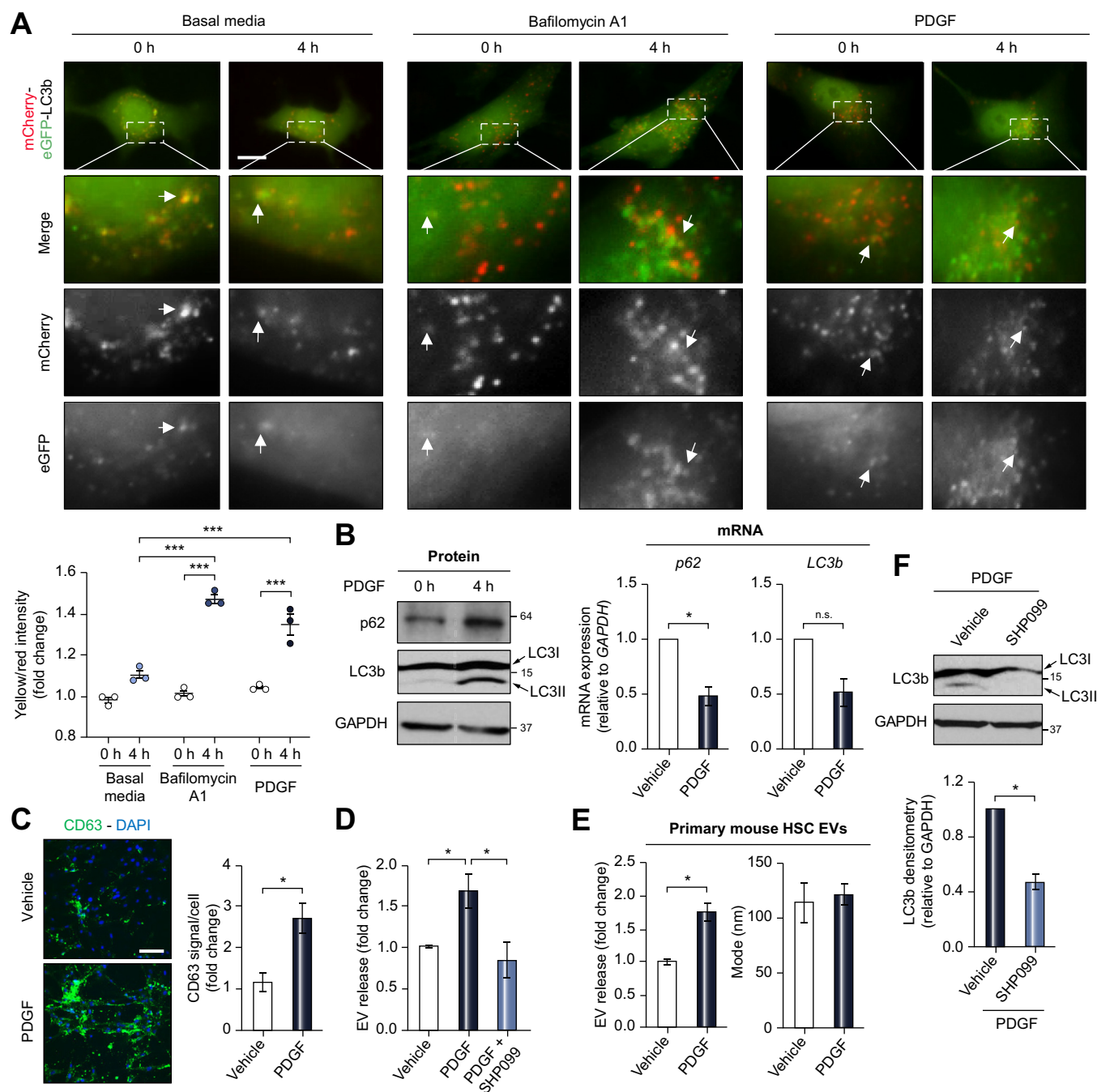


Fig. 1. Inhibition of autophagy correlates with increased EV release in HSCs. (A) LX2 cells were transfected with mCherry-eGFP-LC3b plasmid and cultured in basal media, in the presence of bafilomycin A1 or PDGF for 0–4 h. Time lapse were recorded utilizing a live cell microscope. The graph represents the quantification of mCherry and eGFP signals utilizing ZEN2. (Scale bar: 20 μ m, $n = 3$, paired t test). (B) Primary human HSCs cultured in the presence of PDGF for 0 and 4 h were examined by WB (left) and qPCR (right) for p62 and LC3b. ($n = 4$, Mann-Whitney test). (C) Primary human HSCs treated with PDGF for 12 h were examined by CD63 immunostaining. Fluorescence was quantified utilizing ImageJ. (Scale bar: 100 μ m, $n = 5$, Mann-Whitney test). (D) EVs derived from primary human HSCs treated with vehicle, PDGF or PDGF+SHP099 for 12 h were analyzed by NTA ($n = 3$, one-way ANOVA with Bonferroni comparison). (E) EVs derived from primary mouse HSCs treated with PDGF for 12 h were analyzed by NTA. ($n = 3$, Mann-Whitney test). (F) Primary human HSCs cultured in the presence of PDGF or PDGF+SHP099 for 12 h were examined by WB for LC3b and quantified by densitometry. ($n = 6$, Mann-Whitney test). Graph bars represent SEM, * $p < 0.05$, *** $p < 0.001$. EV(s), extracellular vesicle(s); HSC(s), hepatic stellate cell(s); NTA, Nanoparticle-Tracking Analysis; WB, western blot.

EV release is regulated by the autophagy activator REDD1

We used this PDGF/SHP2 model to further investigate how autophagy inhibits fibrogenic EV release. For this purpose, we performed HSC whole transcriptome RNA sequencing. Primary

human HSCs were treated with PDGF+SHP099, mRNA was examined by sequencing and RNA sequencing results were analyzed by ingenuity pathway analysis (Qiagen) (Fig. 2). Nearly 25% of the genes were upregulated by SHP099 (Fig. 2A). Several

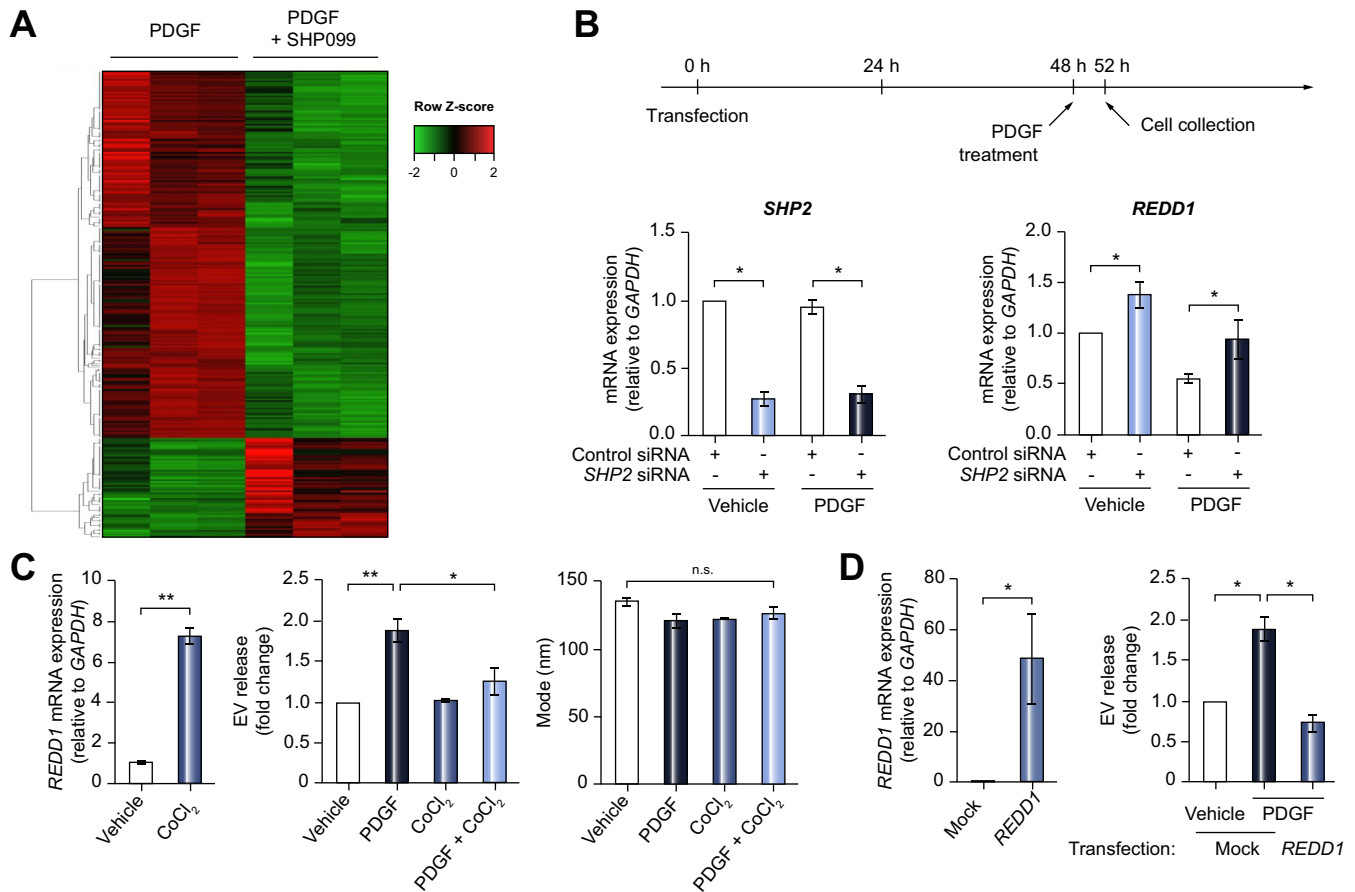


Fig. 2. SHP2 induces EV release by inhibiting REDD1 expression, an mTOR inhibitor. (A) Primary human HSCs were treated with PDGF \pm SHP099 for 48 h and differential gene expression was analyzed by RNA sequencing. Green: downregulated genes, red: upregulated genes. (n = 3). (B) Primary human HSCs were transfected with control or SHP2 siRNA. PDGF was added 48 h later and cells were cultured for additional 4 h. The mRNA levels of *SHP2* and *REDD1* were assessed by qPCR. (n = 3). (C) Primary human HSCs were cultured in the presence of vehicle or CoCl₂ 1 h prior to vehicle or PDGF treatment. *REDD1* mRNA expression was examined by qPCR (left graph, paired *t* test). EV concentration and mode were examined by NTA (middle and right graphs). (n = 3). (D) LX2 cells were transfected with *REDD1* plasmid and 2 days later they were treated with vehicle or PDGF for 12 h. *REDD1* overexpression was examined by qPCR (left graph, paired *t* test). EV concentration was measured by NTA. (n = 3). Graph bars represent SEM, one-way ANOVA with Bonferroni comparison, **p* < 0.05, ***p* < 0.01, n.s., not significant. EV(s), extracellular vesicle(s); HSC(s), hepatic stellate cell(s); NTA, Nanoparticle-Tracking Analysis; qPCR, quantitative PCR.

pathways were affected by SHP2 inhibition, the top one being osteoarthritis (Fig. S3A–B), a process with many parallels to fibrosis.^{6,22–24} Therefore, the osteoarthritis pathway candidates were further confirmed by quantitative PCR (Fig. S3C). As a result, the endogenous inhibitor of mTOR named REDD1 was one of the top targets of SHP2. In prior studies, mTOR promoted liver injury and fibrosis,^{6,25} and inhibited autophagy.²⁶ Here, PDGF repressed REDD1 expression which was restored by SHP2 inhibition (Fig. S3C). As a control, TGF β did not decrease REDD1, suggesting that REDD1 is specifically regulated by the PDGF/SHP2 axis (Fig. S3C). As further confirmation, SHP2 knockdown by siRNA led to REDD1 upregulation following both vehicle and PDGF treatment (Fig. 2B). These results demonstrate that REDD1, an mTOR inhibitor and autophagy activator,^{27,28} is down-regulated by PDGF and SHP2, suggesting a role for REDD1 in EV release.

Next, we aimed to understand the role of REDD1 in liver fibrosis and HSC-derived EV release by stimulating its expression. For this purpose, we utilized the REDD1 stimulator, cobalt chloride (CoCl₂) (Fig. 2C, left).²⁹ Primary human HSCs were treated with CoCl₂ in the presence of vehicle or PDGF. EVs were

examined by NTA. REDD1 expression attenuated PDGF-mediated EV release (Fig. 2C, middle) with no effect on the EV size (Fig. 2C, right). Next, we overexpressed REDD1 in LX2 cells (Fig. 2D, left). Consistent with the previous results, overexpression of REDD1 significantly reduced HSC-derived EV release (Fig. 2D, right). In summary, these results demonstrate that REDD1, an autophagy activator and mTOR inhibitor, is a negative regulator of HSC-derived fibrogenic EV release.

mTOR signaling increases HSC-derived EV release by inhibiting autophagy and activating ROCK1

To further understand how autophagy impacts fibrogenic EV release, we examined the role of the autophagy inhibitor mTOR in HSC-derived EV release. Primary human HSCs were treated with vehicle or PDGF in the presence or absence of rapamycin, a specific mTOR complex 1 (mTORC1) inhibitor.⁶ The effect of rapamycin on mTOR signaling was confirmed by the decrease in ribosomal protein S6 kinase (S6K) phosphorylation, a canonical downstream signaling molecule of mTORC1, while the effect of PDGF was confirmed by the downregulation of PDGFR α protein level (Fig. 3A). In line with our previous results (Fig. 2C–D),

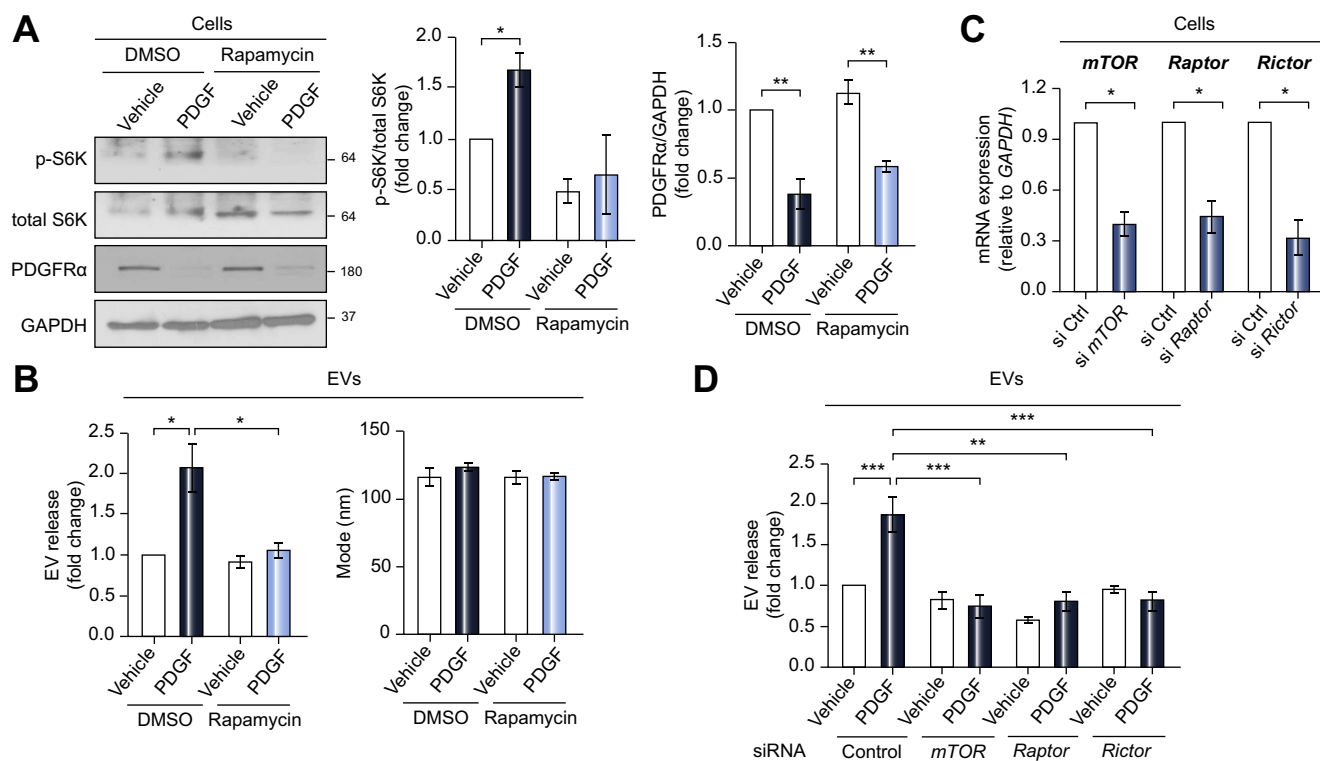


Fig. 3. PDGF-mediated EV release is dependent on mTOR, an autophagy inhibitor. Primary human HSCs were treated with rapamycin for 1 h. PDGF was added, and cells were cultured for an additional 12 h. (A–C, $n = 3$). (A) Whole cell lysates were examined by WB for p-S6K, total-S6K and PDGFR α and quantified by densitometry. (B) EV release and EV mode were measured by NTA. Primary human HSCs were transfected with control, mTOR, Raptor or Rictor siRNA (siControl, si mTOR, si Raptor or si Rictor, respectively). PDGF was added 48 h later and cells were cultured for an additional 12 h. (C–D, $n = 3$). (C) mRNA levels of mTOR, Raptor and Rictor were measured by qPCR (paired t test). (D) EV release was quantified by NTA. Graph bars represent SEM, one-way ANOVA with Bonferroni comparison, * $p < 0.05$, ** $p < 0.01$, *** $p < 0.001$. EV(s), extracellular vesicle(s); HSC(s), hepatic stellate cell(s); NTA, Nanoparticle-Tracking Analysis; WB, western blot.

mTOR inhibition by rapamycin attenuated PDGF-mediated EV release without any effect on EV size, as demonstrated by NTA (Fig. 3B). We then performed mTOR silencing, as well as silencing of mTOR binding partners, regulatory-associated protein of mTOR (Raptor) and rapamycin-insensitive companion of mTOR (Rictor) on primary human HSCs (Fig. 3C). In addition, mTOR knockdown by siRNA abolished PDGF-mediated EV release (Fig. 3D). A similar effect was also obtained with Raptor or Rictor siRNA-mediated knockdown (Fig. 3D), confirming that mTOR signaling promotes EV release.

Next, we examined the origin of mTOR-dependent EV release in primary human HSCs. Since MVBs, the origin of exosomes, can be degraded by autophagy and mTOR is an autophagy inhibitor, we investigated the role of mTOR signaling on exosome release. In our system, PDGF increased p62 protein levels, which were attenuated by rapamycin (Fig. 4A), suggesting that PDGF inhibited autophagy through mTOR. Moreover, autophagy inhibition by bafilomycin A1 (Fig. 4B) or autophagy-related 5 siRNA (Fig. S4) significantly increased the exosome marker CD81 in the purified EV fraction, as well as the microvesicle marker Arf6⁸ (Fig. S5). Based on these results, we investigated the role of mTOR signaling on the MVB pool in primary human HSCs, where CD63 is an MVB and exosome marker. Treatment of cells with PDGF increased the MVB pool, which was abolished by rapamycin, as demonstrated by immunofluorescence (Fig. 4C). In line with this, rapamycin reduced PDGF-mediated exosome release, as demonstrated by decreased CD81 and CD63 protein levels in the

EV fraction (Fig. 4D). These results suggest that mTOR signaling induces exosome release.

In contrast to exosomes, microvesicle release is dependent on ROCK1 activity.^{11,30,31} Therefore, we next investigated the effect of mTOR signaling on ROCK1 activity and microvesicle release. PDGF treatment of primary human HSCs activated ROCK1 signaling as demonstrated by the increased levels of the phosphorylated ROCK1 downstream signaling molecule, myosin phosphatase target subunit 1 (MYPT1) (Fig. 4E). This was abolished by treating HSCs with the ROCK1 inhibitor, fasudil (Fig. 4E). Subsequently, ROCK1 inhibition by fasudil significantly decreased PDGF-mediated EV release, as demonstrated by the microvesicle marker Arf6 (Fig. S5) and the exosomal marker CD81 (Fig. 4B), suggesting crosstalk between the mechanisms of exosome and microvesicle release. PDGF-mediated ROCK1 activity was also inhibited by rapamycin, as demonstrated by the attenuated MYPT1 phosphorylation (Fig. 4F) suggesting that PDGF induced ROCK1 activation through mTOR. Furthermore, rapamycin reduced PDGF-mediated microvesicle release as demonstrated by decreased Arf6 protein levels in the EV fraction (Fig. 4D). These data suggest that mTOR signaling induces microvesicle release.

In summary, mTOR signaling induces exosome release by inhibiting autophagic degradation of MVBs, and microvesicle release by activating ROCK1 signaling, which provide mechanistic insight into PDGF-mediated fibrogenic EV release.

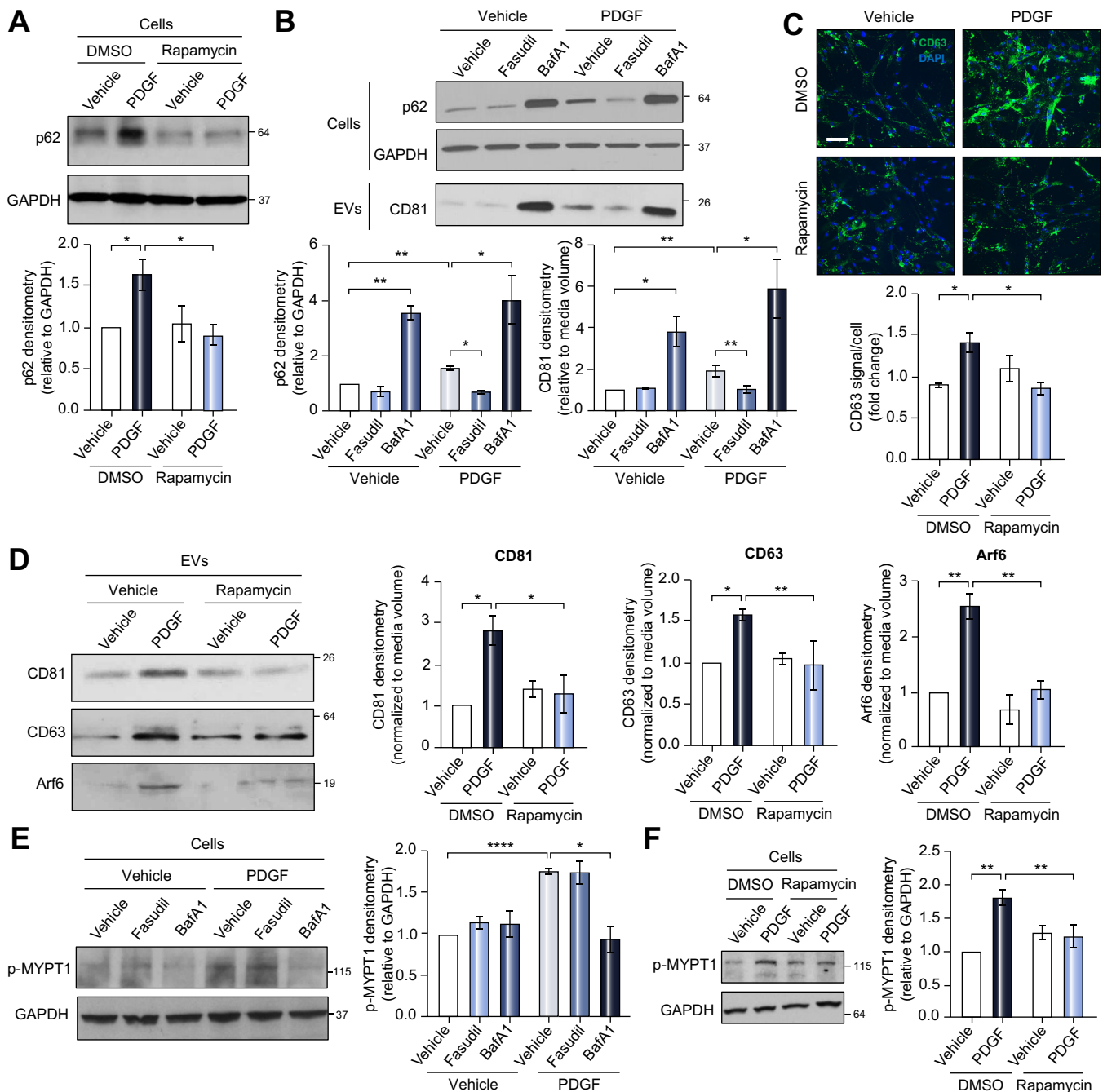


Fig. 4. Autophagy inhibition and ROCK1 activity increase PDGF-mediated EV release. Primary human HSCs were treated with rapamycin, fasudil or bafilomycin A1 for 1 h. PDGF was added and cells were cultured for an additional 12 h. (A) Whole cell lysates were examined by WB for p62 and quantified by densitometry. (n = 9). (B) Whole cell lysates and EVs were examined by WB for p62 (cells) and CD81 (EVs), and quantified by densitometry. (n = 7). (C) CD63 levels were assessed by immunostaining. (Scale bar: 100 μ m, n = 6). (D) EV population was analyzed by WB for CD63, CD81 and Arf6, and quantified by densitometry. (n = 3). (E–F) Whole cell lysates were examined by WB for phosphorylated MYPT1 and quantified by densitometry. (n = 6). Graph bars represent SEM, one-way ANOVA with Bonferroni comparison, * p < 0.05, ** p < 0.01, **** p < 0.0001. EV(s), extracellular vesicle(s); HSC(s), hepatic stellate cell(s); WB, western blot.

mTOR-mediated EVs induce HSC migration *in vitro*

Receptor tyrosine kinase (RTK) signaling is prominent in fibrosis,^{16,32–35} thus we assessed EV content, using a phospho-RTK protein array. We screened for active RTKs which can be transferred from EVs to recipient cells. Primary human HSCs were treated with vehicle, PDGF, rapamycin or PDGF+rapamycin and EVs were collected after 12 h. The results of the array

showed that several phosphorylated RTKs were present in the EVs after PDGF treatment, such as fibroblast growth factor receptor 3 (FGFR3), tunica interna endothelial cell kinase (Tie2), anaplastic lymphoma kinase and receptor tyrosine kinase-like orphan receptor 1 (Fig. 5A). The most upregulated mTOR-dependent kinase (upregulated by PDGF and decreased by rapamycin) was phospho-FGFR3 (Fig. 5A), an RTK involved in

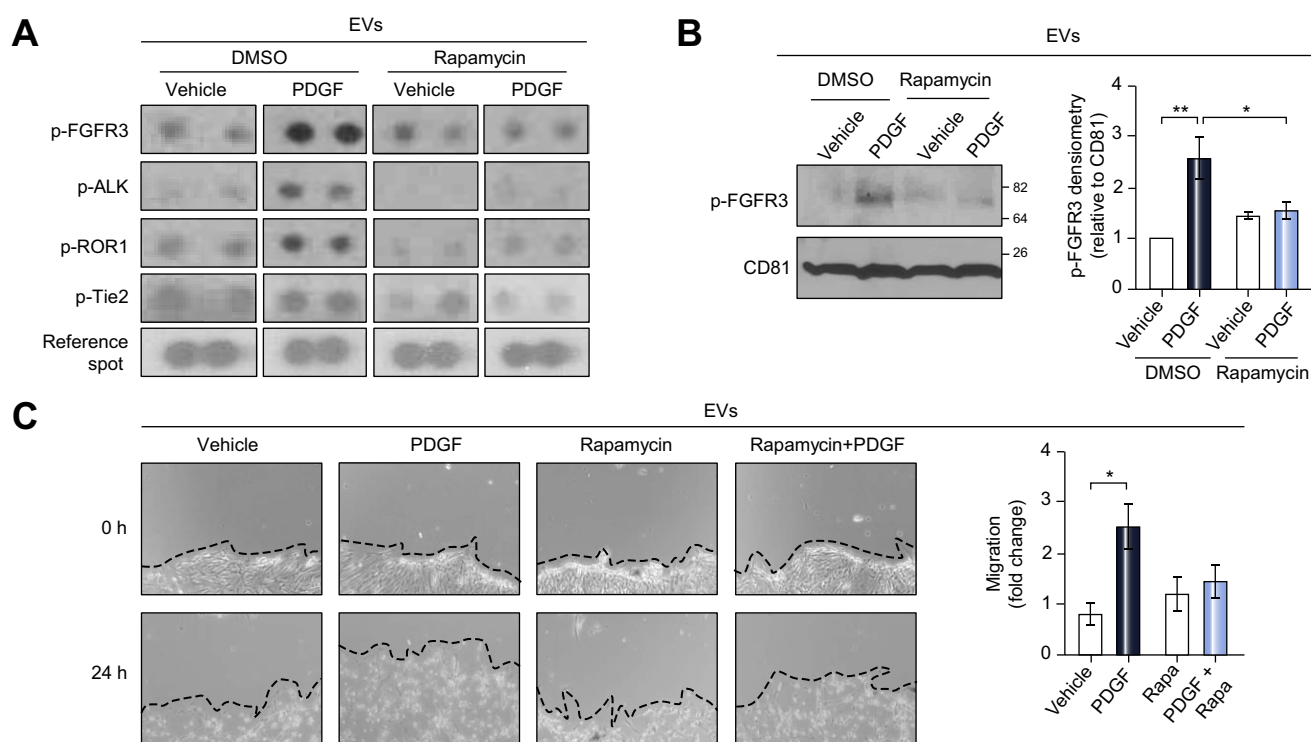


Fig. 5. mTOR-dependent EVs are pro-migratory by transferring phosphorylated RTKs. (A–C) Primary human HSCs were treated with rapamycin for 1 h. PDGF was added, and cells were cultured for an additional 12 h. (A) Equal number of EVs were lysed and analyzed by a phospho-RTK protein array. (n = 3, images cropped). (C) Equal number of EVs were lysed and examined by WB for phosphorylated FGFR3 and CD81, and quantified by densitometry. (n = 3). (D) Confluent HSCs were scratched using a 10 μ l pipette tip. Cells were washed and incubated with donor cell EVs in basal media for 24 h. The migration of cells in 3 pre-selected areas was measured at 0 and 24 h (n = 4). Graph bars represent SEM, one-way ANOVA with Bonferroni comparison * p < 0.05, ** p < 0.01. EV(s), extra-cellular vesicle(s); HSC(s), hepatic stellate cell(s); RTK(s), receptor tyrosine kinase(s); WB, western blot.

fibroblast migration.³⁶ This result was confirmed by performing 2 additional array replicates and by WB (Fig. 5B). These data suggest that mTOR signaling not only promotes the release of the EVs but also mediates their enrichment with activated RTKs. Since the identified RTKs have been previously associated with cell migration,^{36–39} we next examined the effect of these RTK-enriched EVs on HSC migration. Recipient primary human HSCs were plated at confluency, scratched and treated for 24 h with EVs derived from vehicle, rapamycin, PDGF or PDGF+rapamycin-treated HSCs. EVs derived from PDGF-treated cells significantly increased recipient HSC migration, unlike EVs derived from PDGF+rapamycin-treated cells, when compared to EVs from vehicle-treated cells (Fig. 5C). In summary, these results demonstrate that mTOR promotes the release of pro-migratory RTK-enriched EVs.

Deletion of HSC-specific SHP2 decreases liver fibrosis *in vivo*

As SHP2 is an upstream regulator of mTOR-dependent EV release, we examined its levels in patients with liver cirrhosis. In whole liver lysates, SHP2 was increased in patients with liver cirrhosis compared to healthy individuals (Fig. 6A). We utilized a recently published single cell RNA sequencing database⁴⁰ (GEO accession number GSE136103) to examine gene expression in healthy vs. cirrhotic human liver cells. SHP2 was expressed by the majority of liver cells (Fig. S6A). However, PDGFR, an important component in our mechanism, was expressed mainly by mesenchymal cells (HSCs and myofibroblasts) (Fig. S6B). Therefore, we sought to investigate the effect of HSC-specific

Shp2 deletion in liver fibrosis in mice. We crossed *Pdgfrb*^{CreERT2} mice with *Shp2*^{fl/fl} mice to obtain *Pdgfrb*^{CreERT2}/*Shp2*^{fl/fl} mice expressing the chimeric CreERT2 recombinase in PDGFR β ⁺ cells. As a first step, the efficiency of the CreERT2 was confirmed by crossing *Pdgfrb*^{CreERT2} mice with Rosa26-Tomato-STOP-GFP mice where the Tomato sequence is followed by a STOP codon and floxed by loxP sites (Fig. S7). In the progeny, upon tamoxifen administration, in the PDGFR β ⁺ cells CreERT2 enters the nucleus and deletes the Tomato-STOP sequence leading to GFP expression, while in the other cells only the Tomato gene is expressed (Fig. S7). We identified that GFP⁺ cells were situated in a non-parenchymal position (Fig. S8A–B). We confirmed by α -smooth muscle actin (α SMA) immunofluorescence that 74% of α SMA⁺ HSCs in the liver express the CreERT2 (Fig. S8C).

Next, we examined the effect of HSC-specific SHP2 deletion on the establishment of liver fibrosis, which was induced by CCl₄ administration for 6 weeks. Livers were then collected and analyzed by Sirius red and WB. As expected, hepatic collagen I, α SMA protein levels, and Sirius red staining were increased in littermate control mice (*Shp2*^{fl/fl}) after chronic CCl₄ (Fig. 6B–C). However, hepatic fibrosis was significantly reduced when the *Shp2* gene was deleted selectively in HSCs (*Shp2*^{ΔHSC} mice), as demonstrated by protein levels of collagen I, α SMA, and Sirius red staining (Fig. 6B–C). In addition, circulating EVs were examined for p-FGFR3 level, which was not different across the groups (Fig. S9). To test for intermediate level effects, we utilized *Shp2*^{Δ^{WT}} heterozygous mice. In this model, the deletion of only 1 allele of *Shp2* was sufficient to reduce liver fibrosis (Fig. S10). As a

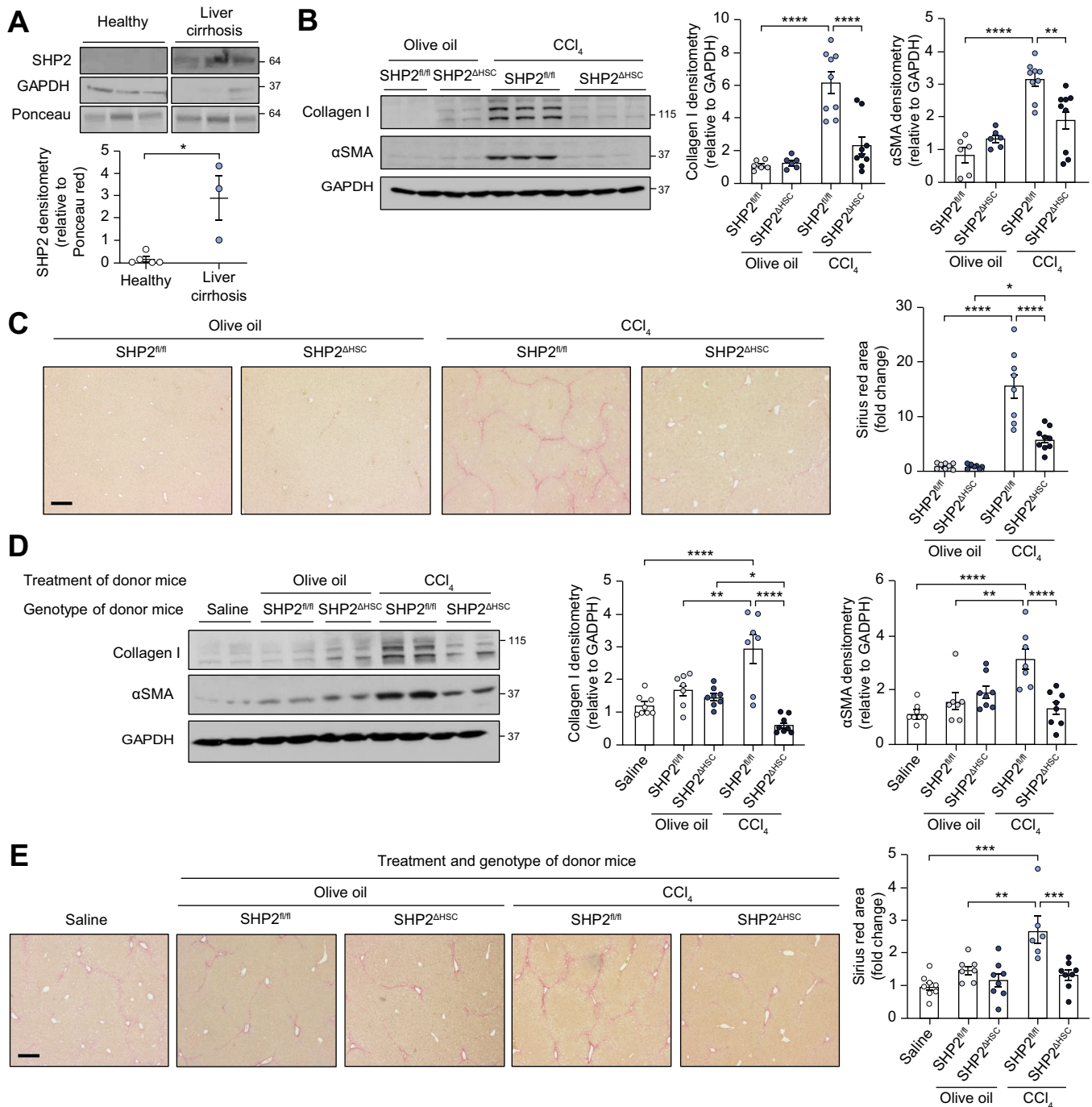


Fig. 6. *Shp2* deletion selectively in HSCs reduces liver fibrosis. (A) Patient liver samples were lysed and analyzed by WB. 3–5 patients/group, WB images cropped from the same blot, graph bars represent SEM, * $p < 0.05$ Mann-Whitney test. (B–C) *Shp2*^{fl/fl} or *Shp2*^{ΔHSC} male and female mice were treated with either olive oil or CCl₄ for 6 weeks. Livers were analyzed by WB (C) and Sirius red staining (D). (n = 6–8 animals/group). (D–E) C57Bl/6 male and female mice were treated for 4 weeks with phosphate-buffered saline or equal number of EVs derived from donor mice as indicated in parallel with CCl₄. Livers were analyzed by WB (E) and Sirius red (F) (n = 7–8 animals/group). Scale bars: 20 μ m, graph bars represent SEM, one-way ANOVA with Bonferroni comparison * $p < 0.05$, ** $p < 0.01$, *** $p < 0.001$, **** $p < 0.0001$. CCl₄, carbon tetrachloride; EV(s), extracellular vesicle(s); HSC(s), hepatic stellate cell(s); RTK(s), receptor tyrosine kinase(s); WB, western blot.

second injury model, we performed BDL surgeries on *Shp2*^{ΔHSC} mice or their *Shp2*^{fl/fl} littermate controls. As in the CCl₄ injury model, the *Shp2*^{ΔHSC} mice had significantly reduced fibrosis compared to the control mice after BDL, as demonstrated by Sirius red staining and WB (Fig. S11). In summary, *Shp2* deletion selectively in HSCs significantly attenuates liver fibrosis.

EVs from mice with HSC-specific SHP2 deletion reduce CCl₄-mediated liver fibrosis in WT mice

We have demonstrated that EVs derived from PDGF-treated HSCs are fibrogenic²⁰ and SHP2 is critical for liver fibrosis (Fig. 6B–C). Therefore, we next investigated how HSC-specific SHP2 influences the fibrogenic potential of circulating EVs and

how these EVs affect fibrosis *in vivo*. First, we examined the cell-specificity of EV uptake. Flag-tagged EVs generated in LX2 cells were administered intraperitoneally to recipient WT mice and livers were examined 24 h later by double immunofluorescence staining. The results demonstrate co-localization of EVs with HSCs, macrophages and endothelial cells, suggesting EV uptake by these cell types (Fig. S12). Next, donor mice, *Shp2*^{ΔHSC} mice or *Shp2*^{fl/fl} littermate controls, received either olive oil or CCl₄ for 6 weeks followed by isolation of circulating EVs. The concentration of small EVs in a mouse circulation is 10¹⁰ EVs/ml (Fig. S13A). To avoid potential side effects by overloading the mice with a high amount of EVs, saline or 2x10⁸ EVs from each donor group were transplanted into WT mice daily by intraperitoneal injections in conjunction with CCl₄ for 4 weeks (Fig. S13B). Compared to saline administration, EVs from olive oil-treated *Shp2*^{fl/fl} or *Shp2*^{ΔHSC} donor mice did not affect liver fibrosis. However, EVs from CCl₄-treated *Shp2*^{fl/fl} control mice significantly increased CCl₄-induced liver fibrosis, as demonstrated by WB and Sirius red (Fig. 6D–E), suggesting that these EVs are fibrogenic. Furthermore, EVs isolated from CCl₄-treated *Shp2*^{ΔHSC} mice significantly reduced CCl₄-induced liver fibrosis (Fig. 6D–E), suggesting that the deletion of SHP2 selectively in HSCs reduces the fibrogenic potential of the EVs. In summary, SHP2 deletion selectively in HSCs significantly attenuates the fibrogenic profile of circulating EVs.

Discussion

This study identified a novel mechanism involving autophagy as an essential process regulating fibrogenic EV release from HSCs in liver fibrosis. We discovered a new role for REDD1, an endogenous inhibitor of mTOR signaling, in the repression of fibrogenic EV release. We demonstrated that by inhibiting autophagy and activating ROCK1 signaling mTOR signaling is crucial for the release of HSC-derived pro-migratory EVs. Inhibition of autophagy leads to the release of MVB content as exosomes, while the activation of ROCK1 signaling leads to the release of plasma membrane-derived microvesicles. Furthermore, we provide evidence that mTOR-mediated EVs are pro-migratory *in vitro*. Finally, blocking this mechanism *in vivo* attenuates circulating pro-fibrotic EVs and liver fibrosis in mice (Fig. 7).

Autophagy is proposed to induce HSC activation by degrading lipid droplets. This process is mediated by a specific type of selective autophagy called lipophagy.⁴¹ Consistently, TGFβ can increase autophagy flux in lung fibroblasts.⁴² However, the importance of autophagy to numerous cellular mechanisms clouds its canonical categorization as a pro- or anti-fibrotic process. In hepatocytes, autophagy has been described as an anti-fibrogenic pathway since it generates survival signals for hepatocytes.² A recent study demonstrated that in alcohol-related liver disease, inhibition of autophagy in hepatocytes is linked to increased EV release.⁴³ Nevertheless, the exact mechanism of autophagy-dependent EVs, especially in HSCs and liver fibrosis, remains elusive. In our system, we revealed that PDGF- and SHP2-, but not TGFβ, mediated activation of HSCs decreased autophagy, which correlated with an increase in fibrogenic EV release. Consistently, inhibition of autophagy enhanced EV release. Taken together these results demonstrate that, unlike TGFβ stimulation, autophagy is inhibited in PDGF-stimulated HSCs leading to enhanced EV release.

A canonical autophagy inhibitor is mTOR,²⁶ which is also reported to inhibit lysosomal degradation.⁴⁴ Moreover, autophagy

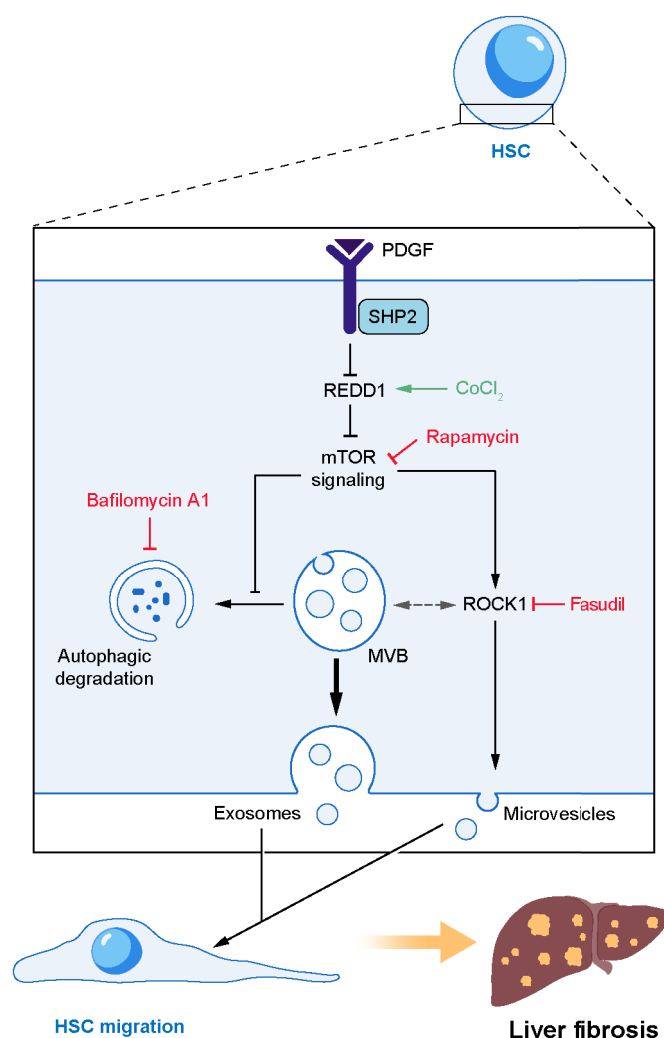


Fig. 7. Approaches to inhibit pro-fibrotic mTOR-mediated EV release. In HSCs, PDGF and SHP2 repress REDD1 expression to amplify mTOR signaling. In turn, mTOR induces exosome release by inhibiting MVB autophagic degradation and microvesicle release by activating ROCK1 signaling. These exosomes and microvesicles induce other HSC migration leading to an amplification of the pro-fibrotic signals and *in vivo* liver fibrosis. In this schema, CoCl₂ stimulates REDD1 expression, rapamycin inhibits mTOR, bafilomycin A1 inhibits autophagic degradation and fasudil inhibits ROCK1 signaling. HSC(s), hepatic stellate cell(s); MVB, multivesicular body.

can be activated by the mTOR endogenous inhibitor REDD1, which mainly inhibits the mTORC1 downstream effector p-S6K.²⁸ It has been shown that SHP2, the PDGF downstream signaling molecule, activates mTOR signaling in cardiomyocytes.⁴⁵ Herein, we made the novel observation of REDD1 as a link between SHP2 and mTOR in HSCs and liver fibrosis. We demonstrated that PDGF and SHP2 repressed the inhibitor of mTOR, REDD1, supporting increased mTOR signaling and EV release. EVs derived from cancer cells have been reported to activate mTOR signaling in recipient cells.⁴⁶ Nevertheless, the mechanism by which mTOR signaling affects EV release in the donor cells remains unknown. In our study, we revealed that, in HSCs, mTOR signaling induced exosome release by inhibiting MVB degradation. Moreover, we found that mTOR induced ROCK1 activity, which led to HSC-derived microvesicle release,

consistent with the known role of ROCK1 in inducing microvesicle release by hepatocytes.¹¹ These results indicate that mTOR induces both exosome and microvesicle release by simultaneously inhibiting autophagy and activating ROCK1 (Fig. 7).

mTOR and SHP2 play important roles in cancer by stimulating cell proliferation and migration.^{47–49} However, the utilization of inhibitors has given divergent results^{50,51} possibly due to cell heterogeneity and cell specific effects. Previously, it has been demonstrated that SHP2 disruption suppresses fibroblast activation and exerts an anti-fibrotic role in dermal and pulmonary fibrosis.¹⁹ Nevertheless, the role of HSC-specific SHP2 in liver fibrosis remains under-evaluated. Here, we demonstrated that inhibiting mTOR signaling in EV donor cells upon pro-migratory PDGF stimulation reduced the enrichment of EVs with activated RTKs and therefore their migratory potential. These activated RTKs, such as FGFR3 and Tie2, are also reported to be involved in fibrosis^{36,52–54} and serve as fibrogenic EV cargos. Along this line, *in vivo* liver fibrosis was attenuated when mice were transplanted with EVs derived from CCl₄-treated *Shp2* conditional knockout mice compared to CCl₄-treated control mice, confirming the fibrogenic potential of SHP2-dependent EVs. Moreover, the deletion of SHP2, upstream of mTOR, selectively in HSCs attenuated circulating fibrogenic EVs and liver fibrosis in both CCl₄ and BDL mouse models. Taken together, these results suggest that blocking the mechanism which leads to pro-migratory and pro-fibrotic EVs attenuates *in vivo* liver fibrosis.

In conclusion, in HSCs, SHP2 promotes fibrosis by inhibiting autophagy and REDD1 and activating the mTOR pathway, thus enhancing the release of fibrogenic EVs. Inhibition of SHP2-mTOR signaling might serve as a novel target in the treatment of liver fibrosis.

Abbreviations

Arf6, ADP ribosylation factor 6; α SMA, α -smooth muscle actin; BDL, bile duct ligation; CCl₄, carbon tetrachloride; EV(s), extracellular vesicle(s); FGF, fibroblast growth factor; HSC(s), hepatic stellate cell(s); mTOR, mammalian target of rapamycin; MVB, multivesicular body; NTA, Nanoparticle-Tracking Analysis; PDGF, platelet-derived growth factor; Raptor, regulatory-associated protein of mTOR; Rictor, rapamycin-insensitive companion of mTOR; ROCK1, Rho-associated protein kinase 1; RTK, receptor tyrosine kinase; S6K, ribosomal protein S6 kinase; SHP2, Src homology 2 domain protein phosphatase 2; siRNA, small interfering RNA; TGF β , transforming growth factor- β ; Tie2, tunica interna endothelial cell kinase; WB, western blotting; WT, wild-type.

Financial support

Supported by the AASLD Foundation Pinnacle Research Award and a Pilot and Feasibility Award from the Mayo Clinic Center for Cell Signaling in Gastroenterology (P30DK084567) (EK), and National Institutes of Health (NIH) USA R01 AA021171 (VHS).

Conflict of interest

The authors declare no conflicts of interest that pertain to this work.

Please refer to the accompanying ICMJE disclosure forms for further details.

Authors' contributions

EK conceived and supervised the study; JG, BW, TMA, ZL, XH, SAC performed experiments; JG, SC analyzed the data; SI provided mice; VHS provided support for conceptualization of the study; JG, VHS and EK wrote the manuscript with input from all the authors.

Acknowledgments

The authors thank Dr. McNiven's, Dr. Gores' and Dr. Malhi's groups, the Mayo Clinic Genomics and Molecular Biology Cores, Animal Facilities and Mayo Clinic Center for Cell Signaling in Gastroenterology, the First Affiliated Hospital of Xi'an Jiaotong University, Shengjing Hospital of China Medical University.

Supplementary data

Supplementary data to this article can be found online at <https://doi.org/10.1016/j.jhep.2020.04.044>.

References

Author names in bold designate shared co-first authorship

- [1] Xu J, Camfield R, Gorski SM. The interplay between exosomes and autophagy - partners in crime. *J Cell Sci* 2018;131:jcs215210.
- [2] Allaire M, Rautou PE, Codogno P, Lotersztajn S. Autophagy in liver diseases: time for translation? *J Hepatol* 2019;70:985–998.
- [3] Ni HM, Chao X, Yang H, Deng F, Wang S, Bai Q, et al. Dual roles of mammalian target of rapamycin in regulating liver injury and tumorigenesis in autophagy-defective mouse liver. *Hepatology* 2019;70:2142–2155.
- [4] Hammoutene A, Biquard L, Lasselin J, Kheloufi M, Tanguy M, Vion AC, et al. A defect in endothelial autophagy occurs in patients with nonalcoholic steatohepatitis and promotes inflammation and fibrosis. *J Hepatol* 2020;72:528–538.
- [5] Weiskirchen R, Tacke F. Relevance of autophagy in parenchymal and non-parenchymal liver cells for health and disease. *Cells* 2019;8:16.
- [6] Neef M, Ledermann M, Saegesser H, Schneider V, Reichen J. Low-dose oral rapamycin treatment reduces fibrogenesis, improves liver function, and prolongs survival in rats with established liver cirrhosis. *J Hepatol* 2006;45:786–796.
- [7] Perez de Obanos MP, Lopez Zabalza MJ, Prieto J, Herraiz MT, Iraburu MJ. Leucine stimulates procollagen alpha1(I) translation on hepatic stellate cells through ERK and PI3K/Akt/mTOR activation. *J Cell Physiol* 2006;209:580–586.
- [8] Hirsova P, Ibrahim SH, Verma VK, Morton LA, Shah VH, LaRusso NF, et al. Extracellular vesicles in liver pathobiology: small particles with big impact. *Hepatology* 2016;64:2219–2233.
- [9] Eguchi A, Kostallari E, Feldstein AE, Shah VH. Extracellular vesicles, the liquid biopsy of the future. *J Hepatol* 2019;70:1292–1294.
- [10] Eguchi A, Lazaro RG, Wang J, Kim J, Povero D, Williams B, et al. Extracellular vesicles released by hepatocytes from gastric infusion model of alcoholic liver disease contain a MicroRNA barcode that can be detected in blood. *Hepatology* 2017;65:475–490.
- [11] Hirsova P, Ibrahim SH, Krishnan A, Verma VK, Bronk SF, Werneburg NW, et al. Lipid-induced signaling causes release of inflammatory extracellular vesicles from hepatocytes. *Gastroenterology* 2016;150:956–967.
- [12] Verma VK, Li H, Wang R, Hirsova P, Mushref M, Liu Y, et al. Alcohol stimulates macrophage activation through caspase-dependent hepatocyte derived release of CD40L containing extracellular vesicles. *J Hepatol* 2016;64:651–660.
- [13] Edgar JR, Manna PT, Nishimura S, Banting G, Robinson MS. Tetherin is an exosomal tether. *Elife* 2016;5:e17180.
- [14] Villarroya-Beltri C, Baixauli F, Mittelbrunn M, Fernandez-Delgado I, Torralba D, Moreno-Gonzalo O, et al. ISGylation controls exosome secretion by promoting lysosomal degradation of MVB proteins. *Nat Commun* 2016;7:13588.
- [15] Kostallari E, Shah VH. Pericytes in the liver. *Adv Exp Med Biol* 2019;1122:153–167.
- [16] Kikuchi A, Monga SP. PDGFRalpha in liver pathophysiology: emerging roles in development, regeneration, fibrosis, and cancer. *Gene Expr* 2015;16:109–127.

- [17] Mederacke I, Hsu CC, Troeger JS, Huebener P, Mu X, Dapito DH, et al. Fate tracing reveals hepatic stellate cells as dominant contributors to liver fibrosis independent of its aetiology. *Nat Commun* 2013;4:2823.
- [18] Bazenet CE, Gelderloos JA, Kazlauskas A. Phosphorylation of tyrosine 720 in the platelet-derived growth factor alpha receptor is required for binding of Grb2 and SHP-2 but not for activation of Ras or cell proliferation. *Mol Cell Biol* 1996;16:6926–6936.
- [19] Zehender A, Huang J, Gyorfi AH, Matei AE, Trinh-Minh T, Xu X, et al. The tyrosine phosphatase SHP2 controls TGFbeta-induced STAT3 signaling to regulate fibroblast activation and fibrosis. *Nat Commun* 2018;9:3259.
- [20] Kostallari E, Hirsova P, Prasnicka A, Verma VK, Yaqoob U, Wongjarupong N, et al. Hepatic stellate cell-derived platelet-derived growth factor receptor-alpha-enriched extracellular vesicles promote liver fibrosis in mice through SHP2. *Hepatology* 2018;68:333–348.
- [21] N'Diaye EN, Kajihara KK, Hsieh I, Morisaki H, Debnath J, Brown EJ. PLIC proteins or ubiquilins regulate autophagy-dependent cell survival during nutrient starvation. *EMBO Rep* 2009;10:173–179.
- [22] Athwal VS, Pritchett J, Llewellyn J, Martin K, Camacho E, Raza SM, et al. SOX9 predicts progression toward cirrhosis in patients while its loss protects against liver fibrosis. *EMBO Mol Med* 2017;9:1696–1710.
- [23] Frangou E, Chrysanthopoulou A, Mitsios A, Kambas K, Arelaki S, Angelidou I, et al. REDD1/autophagy pathway promotes thromboinflammation and fibrosis in human systemic lupus erythematosus (SLE) through NETs decorated with tissue factor (TF) and interleukin-17A (IL-17A). *Ann Rheum Dis* 2019;78:238–248.
- [24] Roderfeld M. Matrix metalloproteinase functions in hepatic injury and fibrosis. *Matrix Biol* 2018;68–69:452–462.
- [25] Lang AL, Krueger AM, Schneggelberger RD, Kaelin BR, Rakutt MJ, Chen L, et al. Rapamycin attenuates liver injury caused by vinyl chloride metabolite chloroethanol and lipopolysaccharide in mice. *Toxicol Appl Pharmacol* 2019;382:114745.
- [26] Saxton RA, Sabatini DM. mTOR signaling in growth, metabolism, and disease. *Cell* 2017;168:960–976.
- [27] Brugarolas J, Lei K, Hurley RL, Manning BD, Reiling JH, Hafen E, et al. Regulation of mTOR function in response to hypoxia by REDD1 and the TSC1/TSC2 tumor suppressor complex. *Genes Dev* 2004;18:2893–2904.
- [28] Qiao S, Dennis M, Song X, Vadysirisack DD, Salunke D, Nash Z, et al. A REDD1/TXNIP pro-oxidant complex regulates ATG4B activity to control stress-induced autophagy and sustain exercise capacity. *Nat Commun* 2015;6:7014.
- [29] Salsman J, Stathakis A, Parker E, Chung D, Anthes LE, Koskovich KL, et al. PML nuclear bodies contribute to the basal expression of the mTOR inhibitor DDIT4. *Sci Rep* 2017;7:45038.
- [30] Aoki K, Maeda F, Nagasako T, Mochizuki Y, Uchida S, Ikenouchi J. A RhoA and Rnd3 cycle regulates actin reassembly during membrane blebbing. *Proc Natl Acad Sci U S A* 2016;113:E1863–E1871.
- [31] Hannemann S, Madrid R, Stastna J, Kitzing T, Gasteier J, Schonichen A, et al. The diaphanous-related formin FHOD1 associates with ROCK1 and promotes Src-dependent plasma membrane blebbing. *J Biol Chem* 2008;283:27891–27903.
- [32] Mimche PN, Brady LM, Bray CF, Lee CM, Thapa M, King TP, et al. The receptor tyrosine kinase EphB2 promotes hepatic fibrosis in mice. *Hepatology* 2015;62:900–914.
- [33] Scheving LA, Zhang X, Threadgill DW, Russell WE. Hepatocyte ERBB3 and EGFR are required for maximal CCl4-induced liver fibrosis. *Am J Physiol Gastrointest Liver Physiol* 2016;311:G807–G816.
- [34] Svegliati-Baroni G, Ridolfi F, Di Sario A, Casini A, Marucci L, Gaggiotti G, et al. Insulin and insulin-like growth factor-1 stimulate proliferation and type I collagen accumulation by human hepatic stellate cells: differential effects on signal transduction pathways. *Hepatology* 1999;29:1743–1751.
- [35] Taura K, De Minicis S, Seki E, Hatano E, Iwaisako K, Osterreicher CH, et al. Hepatic stellate cells secrete angiopoietin 1 that induces angiogenesis in liver fibrosis. *Gastroenterology* 2008;135:1729–1738.
- [36] Joannes A, Brayer S, Besnard V, Marchal-Somme J, Jaillet M, Mordant P, et al. FGF9 and FGF18 in idiopathic pulmonary fibrosis promote survival and migration and inhibit myofibroblast differentiation of human lung fibroblasts in vitro. *Am J Physiol Lung Cell Mol Physiol* 2016;310:L615–L629.
- [37] Hasan MK, Nafady A, Takatori A, Kishida S, Ohira M, Suenaga Y, et al. ALK is a MYCN target gene and regulates cell migration and invasion in neuroblastoma. *Sci Rep* 2013;3:3450.
- [38] Saharinen P, Eklund L, Miettinen J, Wirkkala R, Anisimov A, Winderlich M, et al. Angiopoietins assemble distinct Tie2 signalling complexes in endothelial cell-cell and cell-matrix contacts. *Nat Cell Biol* 2008;10:527–537.
- [39] Zhang S, Zhang H, Ghia EM, Huang J, Wu L, Zhang J, et al. Inhibition of chemotherapy resistant breast cancer stem cells by a ROR1 specific antibody. *Proc Natl Acad Sci U S A* 2019;116:1370–1377.
- [40] Ramachandran P, Dobie R, Wilson-Kanamori JR, Dora EF, Henderson BEP, Luu NT, et al. Resolving the fibrotic niche of human liver cirrhosis at single-cell level. *Nature* 2019;575:512–518.
- [41] Hernandez-Gea V, Ghiassi-Nejad Z, Rozenfeld R, Gordon R, Fiel MI, Yue Z, et al. Autophagy releases lipid that promotes fibrogenesis by activated hepatic stellate cells in mice and in human tissues. *Gastroenterology* 2012;142:938–946.
- [42] Racanelli AC, Kikkers SA, Choi AMK, Cloonan SM. Autophagy and inflammation in chronic respiratory disease. *Autophagy* 2018;14:221–232.
- [43] Babuta M, Furi I, Bala S, Bukong TN, Lowe P, Catalano D, et al. Dysregulated autophagy and lysosome function are linked to exosome Production by Micro-RNA 155 in alcoholic liver disease. *Hepatology* 2019;70:2123–2141.
- [44] Liu W, Ye C, Cheng Q, Zhang X, Yao L, Li Q, et al. Macrophage raptor deficiency-induced lysosome dysfunction exacerbates nonalcoholic steatohepatitis. *Cell Mol Gastroenterol Hepatol* 2019;7:211–231.
- [45] Schramm C, Fine DM, Edwards MA, Reeb AN, Krenz M. The PTPN11 loss-of-function mutation Q510E-Shp2 causes hypertrophic cardiomyopathy by dysregulating mTOR signaling. *Am J Physiol Heart Circ Physiol* 2012;302:H231–H243.
- [46] Ghosh AK, Secreto CR, Knox TR, Ding W, Mukhopadhyay D, Kay NE. Circulating microvesicles in B-cell chronic lymphocytic leukemia can stimulate marrow stromal cells: implications for disease progression. *Blood* 2010;115:1755–1764.
- [47] Chen YN, LaMarche MJ, Chan HM, Fekkes P, Garcia-Fortanet J, Acker MG, et al. Allosteric inhibition of SHP2 phosphatase inhibits cancers driven by receptor tyrosine kinases. *Nature* 2016;535:148–152.
- [48] Han T, Xiang DM, Sun W, Liu N, Sun HL, Wen W, et al. PTPN11/Shp2 overexpression enhances liver cancer progression and predicts poor prognosis of patients. *J Hepatol* 2015;63:651–660.
- [49] Matter MS, Decaens T, Andersen JB, Thorgeirsson SS. Targeting the mTOR pathway in hepatocellular carcinoma: current state and future trends. *J Hepatol* 2014;60:855–865.
- [50] Graham L, Banda K, Torres A, Carver BS, Chen Y, Pisano K, et al. A phase II study of the dual mTOR inhibitor MLN0128 in patients with metastatic castration resistant prostate cancer. *Invest New Drugs* 2018;36:458–467.
- [51] Nashan B. mTOR inhibition and clinical transplantation: liver. *Transplantation* 2018;102:S19–S26.
- [52] Guzy RD, Li L, Smith C, Dorry SJ, Koo HY, Chen L, et al. Pulmonary fibrosis requires cell-autonomous mesenchymal fibroblast growth factor (FGF) signaling. *J Biol Chem* 2017;292:10364–10378.
- [53] Mammoto T, Jiang A, Jiang E, Mammoto A. Role of Twist1 phosphorylation in angiogenesis and pulmonary fibrosis. *Am J Respir Cell Mol Biol* 2016;55:633–644.
- [54] Martin-Vilchez S, Rodriguez-Munoz Y, Lopez-Rodriguez R, Hernandez B, Borque-Inurrita MJ, Molina-Jimenez F, et al. Inhibition of tyrosine kinase receptor Tie2 reverts HCV-induced hepatic stellate cell activation. *PLoS One* 2014;9:e106958.